Title: Reduction of Tribocorrosion Products when Using the Platform-Switching Concept

Ghada O Alrabeah [1,2,3], Jonathan C Knowles [2,4,5], and Haralampos Petridis[1]

[1] Prosthodontic Unit, Department of Restorative Dentistry, UCL Eastman Dental Institute, University College London, London, UK

[2] Division of Biomaterials and Tissue Engineering, UCL Eastman Dental Institute, University College London, London, UK

[3] Department of Prosthetic Dental Sciences, College of Dentistry, King Saud University, Riyadh, KSA

[4] Institute of Tissue Regeneration Engineering (ITREN) and Department of Nanobiomedical Science and BK21 Plus NBM, Global Research Center for Regenerative Medicine, Dankook University, 518-10 Anseo-dong, Dongnam-gu, Cheonan, Chungcheongnam-do, Republic of Korea

[5] The Discoveries Centre for Regenerative and Precision Medicine, UCL Campus, Gower Street, LondonWC1E 6BT, United Kingdom

Correspondence:

Dr Ghada O Alrabeah, Prosthodontic Unit, Department of Restorative Dentistry, UCL Eastman Dental Institute, University College London, 256 Gray's Inn Rd, London WC1X 8LD, UK Tel: +44 (0)20 3456 1250; E-mail: g.alrabeah.12@ucl.ac.uk

Dr Haralampos Petridis, Prosthodontic Unit, Department of Restorative Dentistry, UCL Eastman Dental Institute, University College London, 256 Gray's Inn Rd, London WC1X 8LD, UK Tel: +44 (0)20 3456 1250; E-mail: c.petridis@ucl.ac.uk

Key words: dental implants, peri-implantitis, alveolar bone loss, titanium, metal ions, metal nanoparticles

ABSTRACT

The reduced marginal bone loss observed when utilizing the platform-switching concept, may be the result of reduced amounts of tribocorrosion products released to the peri-implant tissues. Therefore, the purpose of this study was to compare the tribocorrosion product release from various platform-matched and platform-switched implant–abutment couplings under cyclic loading. Forty-eight titanium implants were coupled with pure titanium, gold alloy, cobalt-chrome alloy, and zirconia abutments forming either platform-switched or platform-matched groups (n=6). The specimens were subjected to cyclic occlusal forces in a wet acidic environment for 24 hours followed by static aqueous immersion for 6 days. The amount of metal ions released was measured using inductively coupled plasma mass spectrometry. Microscopic evaluations were performed pre- and post-immersion under scanning electron microscope (SEM) equipped with energy dispersive spectroscopy X-ray for corrosion assessment at the interface and wear particle characterization. All platform-switched groups showed less metal ion release compared to their platform-matched counterparts within each abutment material group (P < 0.001). Implants connected to platform-matched cobalt-chrome abutments demonstrated the highest total mean metal ion release (218 ppb) while the least total mean ion release (11 ppb) was observed in the implants connected to platform-switched titanium abutments (P ≤ 0.001). Titanium was released from all test groups with its highest mean release (108 ppb) observed in the implants connected to platform-matched gold abutments (P < 0.001). SEM images showed surface corrosion features such as pitting and bands of fretting scars. Wear particles were mostly titanium ranging from submicron to 48 μm in length. The platform-matched groups demonstrated higher amount of metal ion release and more surface damage. These findings highlight the positive effect of platform-switching concept in the reduction of tribocorrosion products released from dental implants which consequently may minimize the adverse tissue reactions that lead to peri-implant bone loss.

INTRODUCTION

Titanium (Ti) has been the material of choice for dental implants due to its biocompatibility and desirable mechanical properties (Wang and Fenton 1996). Ti is corrosion-resistant under controlled environments and in the absence of load (Gittens et al. 2011). In the hostile oral environment, Ti and other metals used as abutment materials are prone to corrosion (Wennerberg et al. 2004; Alrabeah et al., 2016). Corrosion of dental implants and implants' superstructures may occur as a result of mechanical or electrochemical processes (Gittens et al. 2011). Mechanical loading from occlusal forces leads to micromotion (fretting) between implant and bone (Gilbert et al. 2009; Gittens et al. 2011) and between the implant and its superstructure (Sridhar et al. 2016). The combination of micromotion and a corrosive aqueous medium in the oral cavity, can disrupt the oxide layer protecting the titanium surface and therefore accelerating the corrosion processes (Sridhar et al. 2015; Yu et al. 2015; Alrabeah et al. 2016). The resultant tribocorrosion phenomena, defined as "material deterioration or transformation resulting from simultaneous action of wear and corrosion" (Mischler 2008) leads to the release of metal degradation products which can have deleterious effects to the surrounding peri-implant tissues (Hallab and Jacobs 2009; Noronha Oliveira et al. 2017). Mouhyi et al (Mouhyi et al. 2012) has considered corrosion to be one of the triggering factors leading to peri-implantitis. Peri-implantitis is an osseointegration pathology (Mouhyi et al. 2012; Qian et al. 2012), and stability of the peri-implant bone is a key factor to long term success of dental implants. Decreased peri-implant bone loss has been observed previously when utilizing different approaches related to the connection geometry of the dental implant-abutment interface, such as platform-switching which is defined as "a protocol that includes smaller diameter restorative components that have been placed on larger diameter implant restorative platforms – the outer edge of the implant-abutment interface is horizontally repositioned inwardly and away from the outer edge of the implant platform" (Lazzara and

Porter 2006; Canullo, Fedele, et al. 2010). Several theories have been advocated to explain the concept of platform-switching (Atieh et al. 2010) including the biomechanical stress theory (Maeda et al. 2007) the bacterial theory (Canullo, Quaranta et al. 2010) and the biologic width theory (Hermann et al. 2001). However, the exact aetiology and mechanism behind such enhanced peri-implant bone response has not been confirmed. In a recent study, Alrabeah et al. demonstrated that under static immersion conditions, the amount of metal ions released from platform-matched implant-abutment couplings was greater than platform-switched implants following an accelerated corrosion protocol (Alrabeah et al. 2016). The same authors (Alrabeah et al. 2017) observed an up-regulation in the expression of genes related to bone resorption from osteoblasts in the presence of metal ions released from those implant-abutment couplings. The increase in cytokine levels was more pronounced in the groups containing the corrosion products of platform-matched implants. The authors concluded that altering the implant-abutment connection geometry had an effect on metal ion release which in turn had an effect on osteoblast function and secretion of bone resorbing mediators (Alrabeah et al. 2016, Alrabeah et al. 2017).

The geometry, design, surface chemistry, microstructure, grain size and alloy combination of the implant-abutment interfaces, together with the host environment, are all important factors responsible for the occurrence and severity of different corrosion processes within the complex oral cavity such as pitting, crevice, galvanic and fretting corrosion (Gilbert et al. 2009, Bhola et al. 2011). The existence of such corrosion processes will lead to the release of metal ions and wear particles at various levels depending on the influence these factors. Therefore, the purpose of this study was compare the tribocorrosion product release from various platform-matched and platform-switched implant–abutment couplings under cyclic loading in a wet acidic environment.

MATERIALS AND METHODS:

Preparation of test specimens

  A total of 48 commercially pure titanium (CPTi) dental implants 5x15mm with external hex connection (BAi, Southern Implants, South Africa) were connected to UCLA abutments forming either platform-matched (5mm abutment diameter) or platform-switched (4mm abutment diameter) implant-abutment couplings. The couplings were further divided into four subgroups according to abutment materials: pure titanium (TiCP4: Ti>99.5%; O-0.37%; Fe-0.12%; C-0.05%; other <0.04%), cobalt-chrome alloy (Co-64.76%; Cr-27.51%; Mo-5.46%; Mn-0.67%; Si-0.66%; Fe-0.40%; Ni-0.19%; N-0.19%; other <0.05%), gold alloy (Ceramicor: Au-60%; Pd-20%; Pt-19%; Ir-1%) and zirconium dioxide (zirconia) (ZrO_2 >91%; Y_2O_3-5.25%; Al_2O_3-0.26%; other <0.02%) and therefore forming 8 groups (n=6) as follows: platform-matched titanium abutments (TM), platform-switched titanium abutments (TS), platform-matched cobalt-chrome abutments (CM), platform-switched cobalt-chrome abutments (CS), platform-matched gold abutments (GM), platform-switched gold abutments (GS), platform-matched zirconia abutments (ZM), and platform-switched zirconia abutments (ZS). Titanium, cobalt-chrome and zirconia abutments were prefabricated UCLA abutments from Southern Implants. The gold abutments were UCLA-type gold base from Southern Implants over which high precious gold (Matticast R, Cookson Dental, UK) was cast following manufacturer recommendations. Each implant was embedded in acrylic resin within a plastic container, leaving 1mm of exposed implant surface (fig.1a.). External surfaces of the abutments were coated with commercial resin to limit corrosion to the interfacial area.

Immersion protocol under cyclic loading

Immediately before testing, each embedded implant was connected to its assigned coated abutment using hexed titanium screw, and torqued to 32 Ncm. The assembled sample was placed on a customized 30º inclined stainless-steel jig fixed to the loading instrument. Fresh 1% lactic acid aqueous solution (0.1 mol/l lactic acid and 0.1 mol/l sodium chloride) was prepared immediately before use (pH=2.3) (ISO#10271, 2011). A volume sufficient to produce a ratio of 1ml of solution per 1cm^2 of exposed sample surface area was added to the container.

The samples were subjected to 240.000 cycles of 30º off-axis mechanical loading in a universal hydraulic testing instrument (Dartec HC10, Dartec Limited, UK) for 24 hrs. A maximum load of 100 N was applied according to a sinusoidal curve with frequency of 2.7 Hz. (ISO#14801, 2007) (fig.1a.). During testing, containers were sealed with paraffin film to avoid contamination and evaporation of the solution (fig.1b.).

After 24 hrs of cyclic loading, containers were covered with lid and maintained in an inclined static position using a customized jig (fig.1.c), to insure that the interfaces are completely covered with solution, in an incubator at 37° C for six days under conditions of relatively no motion between sample and solution (ISO#10271, 2011). Overall, the whole aqueous immersion lasted 7 days.

After 7 days, extracts of immersion solution were collected from each container, dissolved in 2% nitric acid, and stored under refrigeration (4°C) until required for elemental analysis.

Quantification of metal ion release

The quantification of metal ions released from the implant-abutment couplings into lactic acid solutions was carried out using Inductively Coupled Plasma-Mass Spectrometry (Varian/Bruker 800-MS Series, Analytical West, Inc., Corona, USA). Elements analyzed were

titanium (Ti), cobalt (Co), chromium (Cr), molybdenum (Mo), zirconium (Zr), yttrium (Y), gold (Au), platinum (Pt) and palladium (Pd).

Examination of the implant and abutment interfaces before and after immersion

Representative specimens from each group were randomly selected for examination of the contacting surfaces before and after immersion under scanning electron microscope (SEM) (FEI, Eindhoven, Netherlands) equipped with energy dispersive spectroscopy x-ray (EDX) (Inca400 EDX, Oxford Instruments Analytical, UK) to assess corrosion and identify any wear particles at the interface. Optical microscopy was also used after testing.

Analysis of wear particles from additional samples

To allow for more wear particle collection and characterization, four additional samples were used. Four implants were connected to platform-matched abutments; one from each material. The mounted samples were subjected to the same loading protocol mentioned earlier, but the immersion solution was neutral 0.9% NaCl in order to observe any particles which would have been digested in the acidic medium of the main experimental groups. After 24 hrs of cyclic loading, the immersion solutions containing corrosion and wear debris were collected, filtered through 0.015μm filter membrane (Nuclepore Track-Etch Membrane, Whatman®, Merck, Germany) and examined under SEM/EDX for wear particle characterization.

Statistical Analysis

Differences in metal ion release between groups were tested by univariate analysis of variance (ANOVA) using SPSS version 22.0 (IBM SPSS Statistics, Tokyo, Japan) ($P<0.05$). Levene's

test of homogeneity of variance was employed (α=0.05). Bonferroni post hoc test was used to analyze significant differences between test groups following the assumption of equal variances (P>0.05). Whereas when equal variances were not assumed (P<0.05) the Dunnett's T3 post hoc test was used. To confirm significant differences between platform-matched and platform-switched groups within each abutment material, t-test for two independent samples was used (P<0.05).

RESULTS

Metal ion release

The order of total metal ions released from test groups from highest to lowest was as follows: CM > GM, CS > ZM, GS > ZS, TM > TS (fig.2a.). All platform-switched groups showed statistically significant decrease in total metal ion release (P<0.001) (fig.2a.) and single element release (P<0.001) (fig. 2b.) compared to their platform-matched counterparts within each abutment material groups (P<0.001) (fig.2a.) except for Au, Pt, and Pd from the gold abutment groups which were minimally released (<1ppb) with no significant difference between GM and GS (P>0.05). Ti ions were released from all test groups with their highest release (108ppb) observed in GM (P<0.001) followed by GS, ZM > CM, ZS,TM > CS, TS in a descending order (fig.2b.).

Pre and post-immersion surface analysis of the implant and abutment interfaces

Post-immersion SEM images showed surface tribocorrosion features such as pitting, cracks, deformation areas, material delamination and fretting scars compared to pre-immersion images (fig.3a. to 3f.). Images of platform-matched groups showed damaged outer implant border in

the form of crooked irregular outer edge unlike the uniform border of platform-switched groups (fig.3g and 3h.), chipped implant edge (fig.3i.) or delamination of surface layer (fig.3j.). In platform-switched groups, fretting lines were limited to the implant surface in contact with the opposing abutment of smaller diameter (fig.3k.)

Post-immersion EDX analysis of abutment surfaces revealed deposition of Ti element from implants onto most abutments (fig.4a.). The surface elemental composition of implants mostly consisted of Ti (fig.4b). There were trace amounts of other elements, such as Zr, Co, Cr and Mo deposited on implant surfaces in low weight % composition (fig.4c.)

SEM images of interfacial surfaces also showed wear particles adherent to implant and abutment surfaces (fig.5a. and 5b.) Wear particles were observed near the hex and were mostly Ti reaching up to 48μm in length (fig.5c.)

Analysis of wear particles in the filtered NaCl extracts

Analysis of the filtered extracts under SEM revealed the presence of numerous particles in the collected NaCl solutions of various compositions and sizes reaching up to 50μm in length (fig.5d and 5e.). EDX analysis of particles revealed their nature to be either metal particles, chlorine crystals or metal particles engulfed within the chlorine crystals (fig.5f.). The majority of wear particles were Ti.

DISCUSSION

The present study has quantitatively and qualitatively assessed tribocorrosion at the interface of different platform-matched and platform-switched implant-abutment couplings by dynamic immersion tests (ISO#10271, 2011). The corrosion test set-up was composed of chemical, galvanic, crevice and fretting/mechanical components. The combination of the above corrosion mechanisms, also termed "tribocorrosion" (Swaminathan and Gilbert 2012), has led to the release of tribocorrosion products in the form of metal ions and particulate debris. Other corrosion tests could include electrochemical testing using potentiodynamic polarization. However, assessment of electrical potential was not performed in the present study because when investigating the biologic effects of corrosion products; element leakage measurement is considered appropriate and clinically relevant (Wataha 2002, Alrabeah et al. 2016). The accelerated tribocorrosion tests were performed in a simplified in-vitro wear simulating an acidic oral environment (ISO#14801, 2007; ISO#10271, 2011). It has been stated that most wear simulation methods lack the scientific evidence to prove that the in vitro simulation corresponds to the in-vivo situation, however, it has been claimed that 1,200,000 cycles in the simulator correspond to 5 years in-vivo (Heintze 2006) and therefore, a total number of 240,000 cycles was chosen in this study to simulate a one year of masticatory clinical service. During mastication, micro-movements occur between prosthetic modular interfaces causing fretting between the implant and abutment contacting surfaces, leading to wear (Souza et al. 2015). Wear particles of various sizes, shapes and compositions have been observed in the present study under SEM either in the collected NaCl solutions or adherent to the contacting surfaces of the implants or abutments. This finding confirms that dental implants may undergo fretting corrosion leading to the release of metal particles to the peri-implant tissues which could explain the appearance of titanium particles in the peri-implantitis biopsies examined by Wilson et al (Wilson Jr et al. 2015). The presence of titanium particles in jaw bones of patients

with dental implants was also confirmed by He et al (He et al. 2016) who showed Ti particles with sizes between 0.5μm and 40μm in the jawbone marrow tissues near the implants. These findings are in accordance with the observations of the present study which revealed particles sizes to be in the range between submicron to 48μm. These metallic particles accumulate in periprosthetic tissues and elicit multinucleated giant cells and bone marrow fibrosis (Schminke et al. 2015; Wilson Jr et al. 2015; He et al. 2016). Particle release was not quantified in the present study neither was the material loss due to wear measured, however, it was evident from the SEM images that fretting features were limited to the contacting surfaces of the implants and abutment. Hence, in the platform-switched implants, the fretting lines on the implant platform were only observed on the surface that was in contact with the opposing smaller diameter abutment, in other words, the 0.5 mm wide circumference of unopposed implant platform, which counts for 20% of the total surface area of the implant platform, was devoid of any fretting lines. Therefore, it could be assumed that if all implant surface in contact with abutment has some forms of fretting features, the platform-switched implants would have 20% less fretting corrosion features than the platform-matched implants. This assumption is supported by the results of the ICP-MS which demonstrated that all platform-switched groups had less metal ion release compared to their platform-matched counterparts. However, it should be noted that fretting corrosion was not the only source for ion release in the present study but rather a combination of other forms of corrosion processes such as chemical, crevice and galvanic corrosion that occurred due to the existence of several factors such as acidic environment, geometry, surface chemistry and alloy combinations of the implant-abutment interfaces.

An increasing number of dental alloys are being utilized as abutment materials in order to improve their clinical performance. However, when dissimilar alloys are placed in direct contact within the wet oral cavity, galvanic corrosion occurs (Chaturvedi 2009; Gittens et al.

2011). Ti behaves differently when connected to different materials; it represents the anodic region in the galvanic cell when connected to a noble metal such as gold, whereas it is considered the cathode when connected to a base metal. The effect of such galvanic phenomena was clearly noted in the results of this study, the more precious the abutment material was, such as in the gold abutment group, the more Ti was released, unlike the gold which was barely released. As the nobility of the abutment material decreased as in the CoCr abutment group, Ti release decreased as it became the cathodic region of the galvanic cell leading to greater release of anodic Co ions. These findings are in agreement with the results of Tuna et al with regards to element release from the implant superstructures (Tuna et al. 2009). Those authors demonstrated that the ion release from the CoCr based abutments was higher than the ion release from the gold based abutments. However, Ti release from the implants was not affected by the abutment material and was relatively the same among all test groups unlike the results of the present study. The reason behind such difference could be due to the differences in test settings (artificial saliva pH=6.7 vs. 1% lactic acid pH=2.3 and potentiodynamic polarisation vs. wet mechanical loading) and differences in the material compositions, grain sizes, surface finish as different implant systems were utilized.

The present study showed that Ti superstructures were superior among all abutment materials tested with regard to total metal ion release (TS=11ppb, TM=30ppb). This finding is in corroboration with the results of Cortada et al. (Cortada et al. 1997; Cortada et al. 2000) who demonstrated that implants coupled with Ti superstructures presented low value of ion release. The authors have considered this ion release (<40ppb) to be very small to cause cytotoxicity (Cortada et al. 1997, Cortada et al. 2000). However, it should be noted that metal particles were observed in the present study under SEM adherent to the interfacial surfaces of the implants and abutments; and if such particles were dissolved, higher values of ions would have been measured. Particles are a source of metal ions since they have large surface area and they are

prone to dissolution resulting in increased ion levels (Hallab et al. 2002). It should also be noted that, although CPTi was the most favourable abutment material in relation to ion release, when implants where connected to platform-matched Ti abutments, the total ion release increased to a level not significantly different from the total ion release of the implants connected to platform-switched zirconia abutments. This observation highlights the great influence of platform-switching on ion release among different materials. Therefore, the interaction of abutment material and size should be considered when selecting implant superstructures in clinical practice. Having said that, the question of "would equal levels of total metal ions but different compositions, as seen in TM and ZS, have the same biological effects?" remains unanswered. Further studies are already being conducted by the current research group, looking into the effect of such various element concentrations on various metabolic pathways related to bone homeostasis.

Biological effects of tribocorrosion products have been widely studied in the orthopeadic literature (Jacobs et al. 2006; Dalal et al. 2012; Ollivere et al. 2012). Hallab and Jacobs have classified the degradation products of orthopaedic implants into two basic types of debris: particles and ionic debris (Hallab and Jacobs 2009). Particulate wear debris range from nanometers to millimetres in size, while metal ions exist in soluble forms bound to serum protein. Both types of degradation debris were observed in the present study at various levels and the biologic response to such tribocorrosion products is of great concern as each type acts biologically through different metabolic pathways (Hallab and Jacobs 2009). It has been reported that the inflammatory response to metal ions or particles is proportional to their concentration (Sun et al. 1997; Agarwal 2004). Significant differences in the concentration of metal ions released from platform-matched and platform-switched implant-abutment couples have been documented in the present study. Based on the analysis of orthopaedic literature regarding the role of implant tribocorrosion products in peri-prosthetic osteolysis, and the

earlier, and ongoing, work of the same research group (Alrabeah et al. 2016, Alrabeah et al. 2017), the authors believe that platform-switching concept has a positive effect in the reduction of tribocorrosion products and therefore suggest that such reduction would lead to less inflammatory cell response, which in turn would lead to less marginal bone loss through different cell metabolic pathways that are still not fully understood.

ACKNOWLEDGEMENTS

REFERENCES

Agarwal S. 2004. Osteolysis—basic science, incidence and diagnosis. Curr Orthopaed. 18(3):220-231.

Alrabeah GO, Brett P, Knowles JC, Petridis H. 2017. The effect of metal ions released from different dental implant-abutment couples on osteoblast function and secretion of bone resorbing mediators. J Dent. 66**:**91-101.

Alrabeah GO, Knowles JC, Petridis H. 2016. The effect of platform switching on the levels of metal ion release from different implant-abutment couples. Int J Oral Sci. 8**:**117-125.

Atieh MA, Ibrahim HM, Atieh AH. 2010. Platform switching for marginal bone preservation around dental implants: a systematic review and meta-analysis. J Periodontol. 81(10): 1350–1366.

Bhola R, Bhola SM, Mishra B, Olson DL. 2011. Corrosion in titanium dental implants/prostheses – a review. Trends Biomater Artif Organs. 25(1):34-36.

Canullo L, Fedele GR, Iannello G, Jepsen S. 2010. Platform switching and marginal bone-level alterations: the results of a randomized-controlled trial. Clin Oral Implants Res. 21:115-121.

Canullo L, Quaranta A, Teles RP. 2010. The microbiota associated with implants restored with platform switching: a preliminary report. J Periodontol. 81(3):403–411.

Chaturvedi TP. 2009. An overview of the corrosion aspect of dental implants (titanium and its alloys). Indian J Dent Res. 20(1):91-98.

Cortada M, Giner L, Costa S, Gil FJ, Rodriguez D, Planell JA. 2000. Galvanic corrosion behavior of titanium implants coupled to dental alloys. J Mater Sci: Materials in Medicine. 11(5): 287-293.

Cortada M, Giner L, Costa S, Gil FJ, Rodriguez D, Planell JA. 1997. Metallic ion release in artificial saliva of titanium oral implants coupled with different metal superstructures. Biomed Mater Eng. 7(3):213-220.

Dalal A, Pawar V, Mcallister K, Weaver C, Hallab N J. 2012. Orthopedic implant cobalt-alloy particles produce greater toxicity and inflammatory cytokines than titanium alloy and zirconium alloy-based particles in vitro, in human osteoblasts, fibroblasts, and macrophages. J Biomed Mater Res. Part A. 100A(8):2147-2158.

Gilbert JL, Mehta M, Pinder B. 2009. Fretting crevice corrosion of stainless steel stem–CoCr femoral head connections: Comparisons of materials, initial moisture, and offset length. J Biomed Mater Res. Part B: Applied Biomater 88B(1):162-173.

Gittens R, Olivares-Navarrete R, Tannenbaum R, Boyan B, Schwartz Z. 2011. Electrical implications of corrosion for osseointegration of titanium implants. J Dent Res. 90(12):1389-1397.

Hallab NJ, Jacobs JJ. 2009. Biologic effects of implant debris. Bull NYU Hosp Jt Dis. 67(2):182.

Hallab NJ, Vermes C, Messina C, Roebuck KA, Glant TT, Jacobs JJ. 2002. Concentration- and composition-dependent effects of metal ions on human MG-63 osteoblasts. J Biomed Mater Res. Part A. 60(3):420-433.

He X, Reichl FX, Wang Y, Michalke B, Milz S, Yang Y, Stolper P, Lindemaier G, Graw M, Hickel R, et al. 2016. Analysis of titanium and other metals in human jawbones with dental implants – A case series study. Dent Mater. 32(8):1042-1051.

Heintze SD. 2006. How to qualify and validate wear simulation devices and methods. Dent Mater. 22(8):712-734.

Hermann JS, Cochran DL, Hermann JS, Buser D, Schenk RK, Schoolfield JD. 2001. Biologic Width around one- and two-piece titanium implants. Clin Oral Implants Res. 12(6):559-71.

ISO#10271. 2011 International Standards Organization: Dentistry — Corrosion test methods for metallic materials; [accessed 22 Feb 2013]. https://www. iso.org/standard/53819.html.

ISO#14801. 2007 International Standards Organization: Dentistry — Implants —Dynamic fatigue test for endosseous dental implants; [accessed 17 Jan 2013]. https://www.iso.org/standard/41034.html.

Jacobs JJ, Hallab NJ, Urban RM, Wimmer MA. 2006. Wear Particles. J Bone Joint Surg Am. 88(Suppl 2):99-102.

Lazzara RJ, Porter SS. 2006. Platform switching: a new concept in implant dentistry for controlling postrestorative crestal bone levels. Int J Periodontics Restorative Dent. 26(1):9-17.

Maeda Y, Miura J, Taki I, Sogo M. 2007. Biomechanical analysis on platform switching: is there any biomechanical rationale? Clin Oral Implants Res. 18(5):581-4.

Mischler S. 2008. Triboelectrochemical techniques and interpretation methods in tribocorrosion: A comparative evaluation. Tribo Int, 41(7):573-583.

Mouhyi J, Dohan Ehrenfest DM, Albrektsson T. 2012. The Peri-Implantitis: Implant Surfaces, Microstructure, and Physicochemical Aspects. Clin Implant Dent Relat Res. 14(2):170-183.

Noronha Oliveira M, Schunemann WVH, Mathew MT, Henriques B, Magini RS, Teughels W, Souza JCM. 2017. Can degradation products released from dental implants affect peri-implant tissues? J Periodontal Res.[accessed 2017 Aug 2]. https://doi.org/10.1111/jre.12479

Ollivere B, Wimhurst JA, Clark IM, Donell ST. 2012. Current concepts in osteolysis. J Bone Joint Surg Br. Series B. 94B(1):10-15.

Qian J, Wennerberg A, Albrektsson T. 2012. Reasons for Marginal Bone Loss around Oral Implants. Clin Implant Dent Relat Res. 14(6):792-807.

Schminke B, Vom Orde F, Gruber R, Schliephake H, Bürgers R, Miosge N. 2015. The pathology of bone tissue during peri-implantitis. J Dent Res. 94(2):354-361.

Souza JCM, Henriques M, Teughels W, Ponthiaux P, Celis JP, Rocha L. 2015. Wear and Corrosion Interactions on Titanium in Oral Environment: Literature Review. Journal of Bio- and Tribo-Corrosion. 1:1-13.

Sridhar S, Abidi Z, Wilson TG, Valderrama P, Wadhwani C, Palmer K, Rodrigues DC. 2016. In vitro evaluation of the effects of multiple oral factors on dental implants surfaces. J Oral Implantol. 42(3):248-257.

Sridhar S, Wilson TG, Palmer KL, Valderrama P, Mathew MT, Prasad S, Acobs M, Gindri IM, Rodrigues DC. 2015. In vitro investigation of the effect of oral bacteria in the surface oxidation of dental implants. Clin Implant Dent Relat Res. 17(S2):e562-e575.

Sun ZL, Wataha JC, Hanks CT. 1997. Effects of metal ions on osteoblast-like cell metabolism and differentiation. J Biomed Mater Res. 34(1):29–37.

Swaminathan V, Gilbert JL. 2012. Fretting corrosion of CoCrMo and Ti6Al4V interfaces. Biomaterials. 33:5487-5503

Tuna SH, Pekmez NO, Keyf F, Canli F. 2009. The electrochemical properties of four dental casting suprastructure alloys coupled with titanium implants. J Appl Oral Sci. 17(5):467-475.

Wang RR, Fenton A. 1996. Titanium for prosthodontic applications: A review of the literature. Quintessence Int. 27(6):401-408.

Wataha JC. 2002. Alloys for prosthodontic restorations. J Prosthet Dent. 87(4): 351–363

Wennerberg A, Ide-Ektessabi A, Hatkamata S, Sawase T, Johansson C, Albrektsson T, Martinelli A, Södervall U, Odelius H. 2004. Titanium release from implants prepared with different surface roughness. Clin Oral Implants Res. 15: 505–512

Wilson Jr TG, Valderrama P, Burbano M, Blansett J, Levine R, Kessler H, Rodrigues DC. 2015. Foreign bodies associated with peri-implantitis human biopsies. J Periodontol. 86(1)**:**9-15.

Yu F, Addison O, Baker SJ, Davenport AJ. 2015. Lipopolysaccharide inhibits or accelerates biomedical titanium corrosion depending on environmental acidity. Int J Oral Sci. 7**:**179-186.

FIGURE LEGENDS

Figure 1: Accelerated tribocorrosion test set-up (a) Schematic of test assembly used for performing the wet tribocorrosion tests. Implant fixtures were embedded so that the 1mm below the interfacial platform area is exposed to the solution and the abutment can be connected. The assembled sample was placed on a customized 30º inclined stainless steel jig. The cyclic load was applied vertically in a unidirectional manner via flat brass indenter to the palatal side of the abutment close to the incisal edge. **(b)** The assemble sample securely fixed to the loading instrument and sealed with paraffin film during cyclic loading for 24 hrs. **(c)** Samples maintained in an inclined static position in the incubator for 6 days after cyclic loading.

Figure 2: Metal ion release from all test groups. **(a)** Total amount of combined metal ions released from different combinations of implant–abutment couplings after 7 days of aqueous immersion in 1% lactic acid solution. **(b)** Ion release for titanium (Ti), cobalt (Co), chromium (Cr), molybdenum (Mo), zirconium (Zr) and yttrium (Y) from the different combinations of implant–abutment couplings after 7 days of aqueous immersion. The results are expressed as mean concentration in parts per billion *(ppb)* ± standard deviation. *n* = 6 per group (*$P<0.001$, **$P<0.05$). TM, Implant connected to platform-matched titanium abutment (5mm); TS,

Implant connected to platform-switched titanium abutment (4mm); CM, Implant connected to platform-matched cobalt-chrome abutment (5mm); CS, Implant connected to platform-switched cobalt-chrome abutment (4mm); GM, Implant connected to platform-matched gold abutment (5mm); GS, Implant connected to platform-switched gold abutment (4mm); ZM, Implant connected to platform-matched zirconia abutment (5mm); and ZS, Implant connected to platform-switched zirconia abutment (4mm).

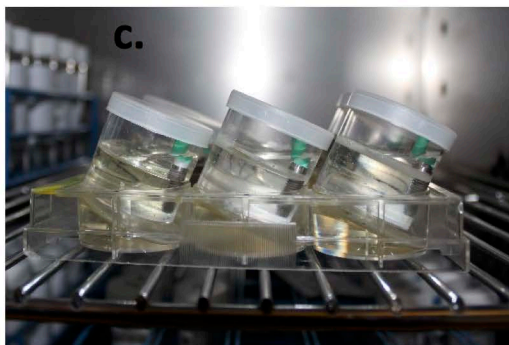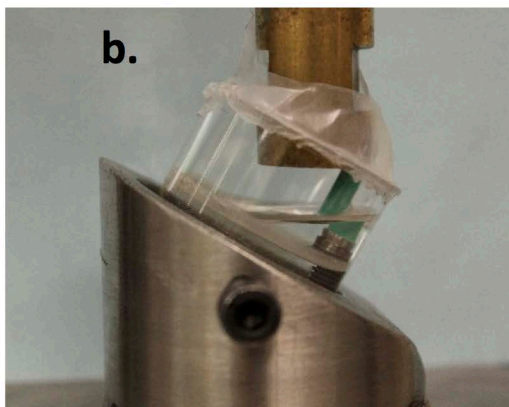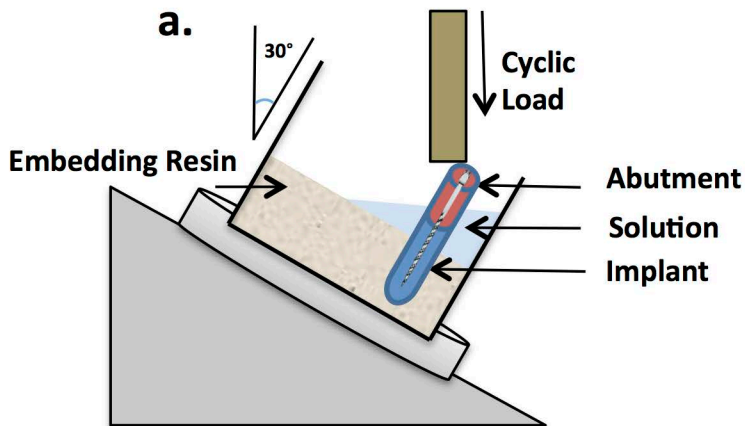**Figure 3: SEM images of the contacting surfaces of different implants and abutments. (a)** Pre-immersion image of a pristine implant showing a uniform machined platform surface (x150) **(b)** Post-immersion image of an implant connected to platform-matched zirconia abutment showing pitting corrosion features as black spots on the interfacial surface (x150), **(c)** Surface crack at the hex area of a platform-switched zirconia abutment (x150) **(d)** Permanent damage of the external hex in the form of burnished surface with material delamination of an implant connected to platform-switched Ti abutment (x150) **(e)** Bands of fretting lines towards the compressed side of an implant connected to platform-matched Ti abutment (x500) **(f)** Implant platform devoid of fretting scars on the side opposite to compression of the same implant of fig.3e (x500) **(g)** Irregular crooked outer border at the compressed side of an implant connected to platform-matched zirconia abutment (x500) **(h)** Uniform outer border at the compressed side of an implant connected to platform-switched zirconia abutment (x500) **(i)** A small shiny metal piece chipped off the outer edge of an implant connected to platform-matched zirconia abutment seen under light microscope. **(j)** Delamination of surface layer near the outer implant platform at the compressed side of an implant connected to platform-matched CoCr abutment. (x50 and x500) **(k)** Post-immersion images of on an implant connected to platform-switched zirconia abutment showing fretting lines confined to the implant platform area in contact with the opposing abutment of smaller
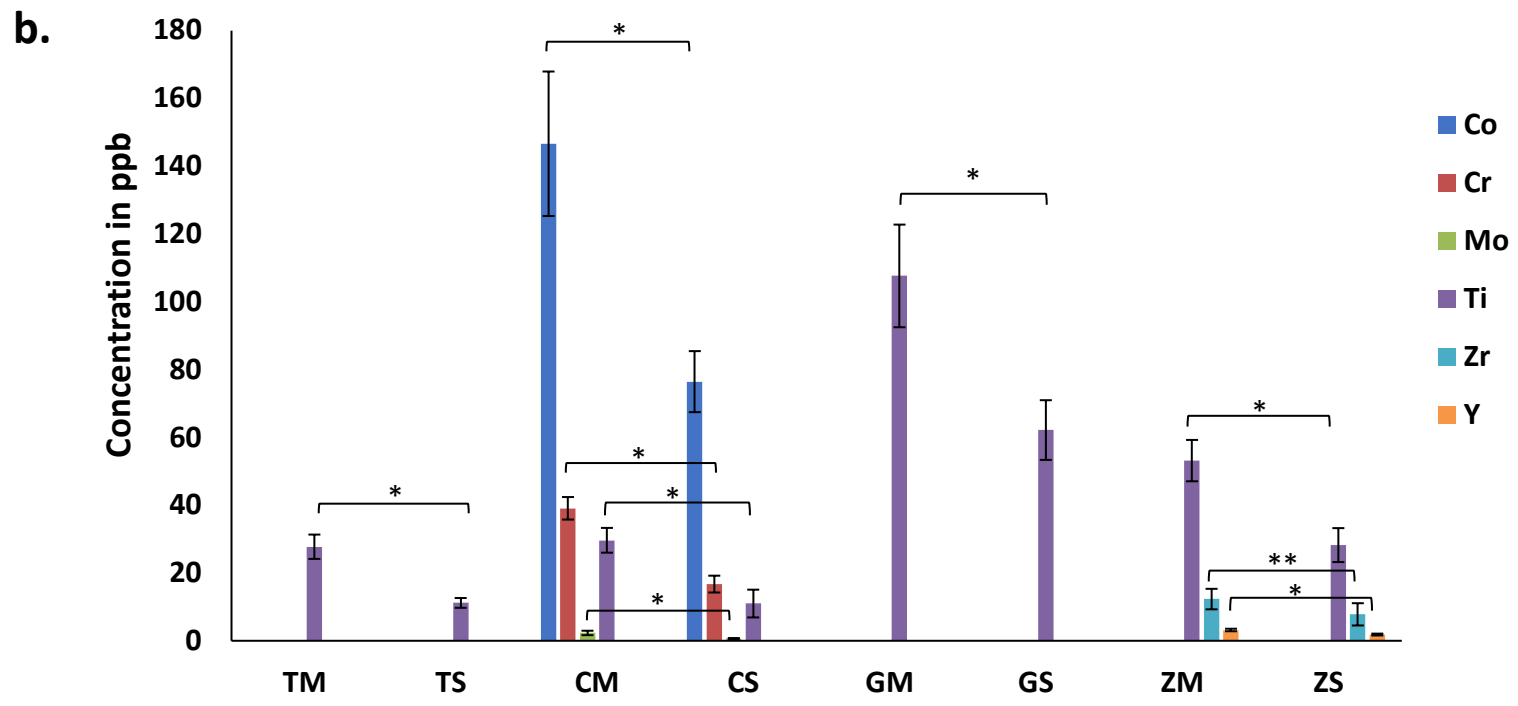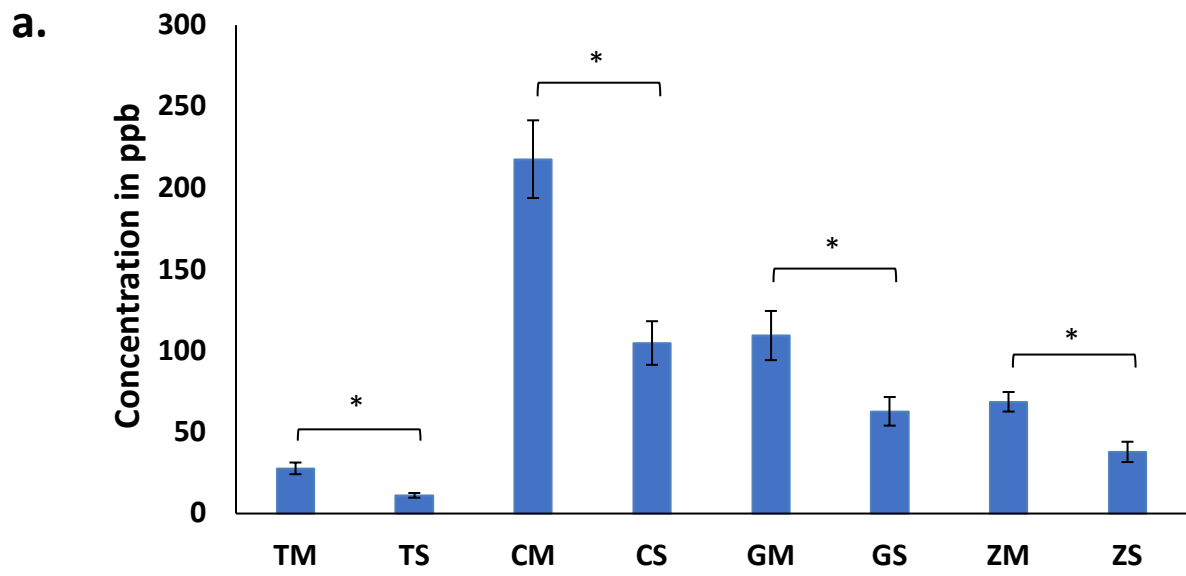
diameter, the area beyond the opposing surfaces was devoid of fretting scars (x80 and x500). SEM, scanning electron microscope

Figure 4: Post immersion EDX elemental analysis of implant-abutment interfaces. (a) Deposition of Ti element from the implants on the inner hex area of a platform-switched gold abutment (x50) **(b)** Implant platform consisting mainly of Ti element on most selected areas of an implant connected to platform-matched gold abutment (x50) **(c)** Deposition of trace amounts of Co, Cr, and Mo on the external hex of an implant connected to platform-matched CoCr abutment (x2000). EDX, energy dispersive spectroscopy x-ray

Figure 5: Post-immersion SEM images and EDX analysis of wear particles on the implant-abutment interfaces and in the filtered extracts of the collected NaCl solutions. (a) Wear particles adherent to the platform surface of an implant connected to platform-matched zirconia abutment. Few particles were composed of Zr indicating their deposition from the abutment into the implant (x250) **(b)** Ti particles adherent to the hex area of a platform-switched gold abutment (x500) **(c)** Ti particle measuring 48 μm in length adherent to a platform-switched CoCr abutment interface (x1000) **(d)** Numerous particles of various sizes and compositions in the filtered NaCl immersion solution of an implant connected to platform-matched zirconia abutment (x100) **(e)** Ti particle measuring 50 μm in length found in the filtered NaCl immersion solution of an implant connected to platform-matched Ti abutment (x1000) (f) Ti and Cr particles engulfed within chlorine crystals found in the filtered NaCl immersion solution of an implant connected to platform-matched CoCr abutment (x1000). SEM, scanning electron microscope; EDX, energy dispersive spectroscopy x-ray

a.

30°

Cyclic Load

Embedding Resin

Abutment

Solution

Implant

b.

c.

a.

b.

-Release of Au, Pt and Pd from GM and GS <1ppb (P>0.05)

a.

Ti: 5.84%	Au: 45.21%
Ca: 3.73%	Pt: 12.40%
Na: 2.65%	Pd: 11.85%
Cl: 2.19%	O: 14.80%
Si: 1.33%	

Spectrum 1

Full Scale 276 cts Cursor: 0.000   keV

b.

Ti: 100%

Spectrum 5

Full Scale 1113 cts Cursor: 0.000   keV

c.

Ti: 75.41%
Co: 15.72%
Cr: 6.72%
Mo: 1.76%
Ca: 0.39%

Spectrum 1

Full Scale 2026 cts Cursor: 0.000   keV